

# Temperature-dependence of spin-polarized transport in ferromagnet / unconventional superconductor junctions

T. Hirai<sup>1,2</sup>, Y. Tanaka<sup>1,2</sup>, N. Yoshida<sup>3</sup>, Y. Asano<sup>4</sup>, J. Inoue<sup>1</sup> and S. Kashiwaya<sup>2,5</sup>

<sup>1</sup> Department of Applied Physics, Nagoya University, Nagoya, 464-8603, Japan

<sup>2</sup> CREST Japan Science and Technology Cooperation (JST) 464-8603, Japan

<sup>3</sup> Department of Microelectronics and Nanoscience, School of Physics and Engineering Physics, Chalmers University of Technology and Goteborg University, S-412 96 Goteborg, Sweden

<sup>4</sup> Department of Applied Physics, Hokkaido University, Sapporo 060-8628, Japan

<sup>5</sup> National Institute of Advanced Industrial Science and Technology, Tsukuba, 305-8568, Japan

(Dated: December 20, 2018)

Tunneling conductance in ferromagnet / unconventional superconductor junctions is studied theoretically as a function of temperatures and spin-polarization in ferromagnets. In *d*-wave superconductor junctions, the existence of a zero-energy Andreev bound state drastically affects the temperature-dependence of the zero-bias conductance (ZBC). In *p*-wave triplet superconductor junctions, numerical results show a wide variety in temperature-dependence of the ZBC depending on the direction of the magnetic moment in ferromagnets and the pairing symmetry in superconductors such as  $p_x$ ,  $p_y$  and  $p_x + ip_y$ -wave pair potential. The last one is a promising symmetry of  $\text{Sr}_2\text{RuO}_4$ . From these characteristic features in the conductance, we may obtain the information about the degree of spin-polarization in ferromagnets and the direction of the *d*-vector in triplet superconductors.

## I. INTRODUCTION

In recent years, transport properties in unconventional superconductor junctions have been studied both theoretically and experimentally. In these junctions, the existence of a zero energy state (ZES)<sup>1,2,3</sup> formed at the interface plays an important role in the tunneling spectroscopy. It is now well known that the zero-bias conductance peak (ZBCP) shows up in tunneling experiments of the high- $T_C$  superconductor junctions<sup>4,5,6,7,8,9</sup> and related phenomena<sup>10,11,12,13,14,15,16,17,18,19,20,21</sup>. Using a tunneling conductance formula in normal-metal / insulator / unconventional superconductor junctions, the origin of ZBCP has been naturally explained in terms of the formation of the ZES.<sup>22,23,24,25</sup> Since the formation of the ZES is a general phenomenon in unconventional superconductor junctions, the ZBCP is also expected in triplet superconductor junctions<sup>26,27,28,29</sup>. Actually, the ZBCP has been observed in  $\text{Sr}_2\text{RuO}_4$ <sup>30,31</sup> and  $\text{UBe}_{13}$ <sup>32</sup>. A possibility of finding the ZBCP has also been theoretically predicted for organic superconductors  $(\text{TMTSF})_2\text{X}$  very recently<sup>33,34,35</sup>.

From a view of future device application, transport properties in hybrid structures consist of ferromagnets and superconductors have attracted attention. It was pointed out in ferromagnet / insulator / spin-singlet unconventional superconductor (*F/I/S*) junctions that the amplitude of the ZBCP decreases with increasing the magnitude of the exchange potential in ferromagnets. This is because the exchange potential breaks the time-reversal symmetry, then suppresses the retro-reflectivity of the Andreev reflection<sup>39,40,41,42,43,44,45,46,47,48</sup>. Thus the ZBCP is sensitive to the degree of spin-polarization in ferromagnets. Since the tunneling conductance is independent of the magnitude of the insulating barrier<sup>49</sup>, it is possible to estimate the spin-polarization in ferromag-

nets through the temperature-dependence in the amplitude of the ZBCP. An experimental test would be carried out in  $\text{La}_{0.7}\text{Sr}_{0.3}\text{MnO}_3/\text{YBa}_2\text{Cu}_3\text{O}_{7-x}$  junctions in near future<sup>50,51,52,53</sup>. When spin-triplet superconductors are attaching to ferromagnets<sup>43,44</sup>, the ZBCP depends not only on the spin-polarization also on another parameters such as the direction of the *d*-vector in triplet superconductors and the direction of the magnetic moment in ferromagnets<sup>45,46</sup>. These unique properties are peculiar to spin-triplet superconductor junctions<sup>36,37</sup>. Thus it may be possible to know details of structures in the pair potential by comparing the characteristic feature in the ZBCP in theoretical calculations and those in experiments<sup>38</sup>.

For this purpose, it is necessary to know relations between the ZBCP and another ingredients such as temperatures and the profile of the pair potential near the junction interface. Although there are several studies on tunneling phenomena in ferromagnet / unconventional superconductor junctions, the temperature-dependence of the conductance has not been clarified in detail yet. In the presence of the ZES, it is known that the amplitude of pair potential is drastically suppressed at a surface or a interface of superconductors<sup>2,28,54,55,56,65</sup>. In the preexisting theories of ferromagnet / unconventional superconductor junctions, however, influences of the spatial dependence in the pair potential on the tunneling conductance remain to be unresolved.

In this paper, we calculate the tunneling conductance in ferromagnet / unconventional superconductor junctions as a function of temperatures and the degree of spin-polarization in ferromagnets, where the spatial dependence of the pair potential is determined self-consistently based on the quasiclassical Green's function theory. In the actual calculations, we choose *d*-wave, and  $p_x + ip_y$ -wave symmetries in the pair potentials which are promising symmetries for high  $T_C$  cuprates and  $\text{Sr}_2\text{RuO}_4$ , re-

spectively. To understand clearly the transport properties in  $p_x + ip_y$ -wave junctions, we compare the results with those in  $p_x$ - and  $p_y$ -wave junctions. From the calculated results, we obtained the following conclusions.

(1) In  $d$ -wave junctions with (110) orientation and  $p_x$ -wave junctions, an incident quasiparticle from a ferromagnet always feels the ZES. In such a situation, the zero-bias tunneling conductance (ZBC) at the zero temperature is insensitive to the barrier potential at the interface. This result indicates a possibility to estimate the magnitude of the spin-polarization in ferromagnets at sufficiently low temperatures by using these junctions in experiments.

(2) In  $d$ -wave junctions with (110) orientation and  $p_x$ -wave junctions, the ZBC monotonically decreases with increasing temperatures for small magnitudes of spin-polarization. On the other hand for large magnitudes of polarization, the ZBC becomes an increasing function of  $T$ . While for  $d$ -wave junctions with (100) orientation and  $p_y$ -wave junctions, where the ZES does not appear, the ZBC is an increasing function of  $T$  independent of the spin-polarization. For  $p_x + ip_y$  junctions, the ZBC first decreases with  $T$  then increases.

(3) For  $p$ -wave junctions, the ZBC has various temperature-dependence depending on the direction of the magnetic moment in ferromagnets. This unique property is peculiar to spin-triplet superconductors.

(4) Throughout this paper, we calculate the ZBC in two ways; i) the spatial dependence of the pair potential is assumed to be the step function (non-SCF calculation) ii) the spatial depletion of the pair potentials is determined self-consistently (SCF-calculation). By comparing results calculated in the two ways, we found that the results in the non-SCF calculation are qualitatively the same with those in the SCF-calculation.

The organization of this paper is as follows. In section 2, we formulate the tunneling conductance with arbitrary angle between the magnetization axis of the ferromagnet and  $c$ -axis of the superconductor. We show the tunneling conductance depends on the direction of the magnetic moments only when superconductors have spin-triplet pairing. In section 3, we calculate the polarization and temperature dependence of ZBC both for  $d$ -wave and  $p$ -wave cases. In section 4, we summarize the obtained results.

## II. FORMULATION

We assume a two-dimensional  $F/I/S$  junction with semi-infinite double-layered structures in the clean limit. A flat interface is perpendicular to the  $x$ -axis and is located at  $x = 0$ . The insulator is modeled by using the delta-functional  $V(x) = H\delta(x)$ , where  $H$  represents the strength of the barrier potential.

The Fermi energy  $E_F$  and the effective mass  $m$  are assumed to be equal in both the ferromagnet and the superconductor. We apply the Stoner model to describe

ferromagnetism through the exchange potential  $U$ . The wave numbers in the ferromagnet for the majority ( $\uparrow$ ) and minority ( $\downarrow$ ) spin are denoted by  $k_{\uparrow(\downarrow)} = \sqrt{\frac{2m}{\hbar^2}(E_F \pm U)}$ . The wave functions  $\Psi(\mathbf{r})$  are obtained by solving the Bogoliubov-de Gennes (BdG) equation under the quasiclassical approximation<sup>57,58</sup>

$$E\Psi(\mathbf{r}) = \int d\mathbf{r}' \tilde{H}(\mathbf{r}, \mathbf{r}')\Psi(\mathbf{r}'), \quad \Psi(\mathbf{r}) = \begin{pmatrix} u_{\uparrow}(\mathbf{r}) \\ u_{\downarrow}(\mathbf{r}) \\ v_{\uparrow}(\mathbf{r}) \\ v_{\downarrow}(\mathbf{r}) \end{pmatrix} \quad (1)$$

$$\tilde{H}(\mathbf{r}, \mathbf{r}') = \begin{pmatrix} \hat{H}(\mathbf{r})\delta(\mathbf{r} - \mathbf{r}') & \hat{\Delta}(\mathbf{r}, \mathbf{r}') \\ \hat{\Delta}^{\dagger}(\mathbf{r}, \mathbf{r}') & -\hat{H}^*(\mathbf{r})\delta(\mathbf{r} - \mathbf{r}') \end{pmatrix},$$

where  $E$  is the energy of a quasiparticle,  $\hat{H}(\mathbf{r}) = h_0\hat{\mathbf{1}} - \mathbf{U}(\mathbf{r})\cdot\boldsymbol{\sigma}(\mathbf{r})$ ,  $h_0 = -\frac{\hbar^2}{2m}\nabla^2 + V(x) - E_F$ ,  $\mathbf{U}(\mathbf{r}) = U\Theta(-x)\mathbf{n}$ ,  $\hat{\mathbf{1}}$  and  $\boldsymbol{\sigma}$  are the  $2 \times 2$  identity matrix and the Pauli matrix, respectively. Here  $\mathbf{n}$  points the direction of the magnetic moment in ferromagnets and  $\Theta(x)$  is the Heaviside step function. The indices  $\uparrow$  and  $\downarrow$  denote the spin degree of freedom of a quasiparticle in superconductors. The configuration of the magnetization axis in ferromagnets and the  $c$ -axis of superconductors are expressed in a polar coordinate  $(\theta_M, \phi_M)$  (see Fig. 1.), where we assume that the quantization axis of spin in the triplet superconductors is parallel to the  $c$ -axis. At first, we assume that the pair potential is a constant independent of  $x$ ,

$$\hat{\Delta}(\theta_S, x) = \hat{\Delta}(\theta_S)\Theta(x), \quad (2)$$

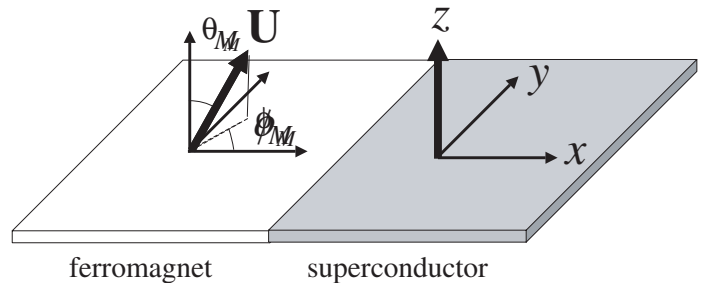


FIG. 1: Schematic illustration of ferromagnet / superconductor junction. The direction of the magnetization axis is denoted by a polar coordinate  $(\theta_M, \phi_M)$ .

where  $\hat{\Delta}(\theta_S)$  does not have the spatial dependence,  $k_x = k_F \cos \theta_S$  and  $k_y = k_F \cos \theta_S$  are the wavenumber in superconductors with  $k_F$  being the Fermi wave number. The pair potential  $\hat{\Delta}(\theta_S)$  is given by

$$\hat{\Delta}(\theta_S) = \begin{pmatrix} \Delta_{\uparrow\uparrow}(\theta_S) & \Delta_{\uparrow\downarrow}(\theta_S) \\ \Delta_{\downarrow\uparrow}(\theta_S) & \Delta_{\downarrow\downarrow}(\theta_S) \end{pmatrix}. \quad (3)$$

The Hamiltonian in Eq. (2) is written in the coordinate of the spin space in the superconductor. It is comprehensive to rewrite the Hamiltonian in the coordinate of spin space in the ferromagnet since this notation is useful to consider the scattering processes. The Hamiltonian in the coordinate of spin space in the ferromagnet is obtained by the following unitary transformation:

$$\tilde{H}_F(\mathbf{r}, \mathbf{r}') = \hat{U}^\dagger \hat{H}(\mathbf{r}, \mathbf{r}') \hat{U} \quad (4)$$

$$\hat{U} = \begin{pmatrix} \hat{U} & 0 \\ 0 & \hat{U}^* \end{pmatrix}, \quad \hat{U} = \begin{pmatrix} \gamma_1 & -\gamma_2^* \\ \gamma_2 & \gamma_1^* \end{pmatrix} \quad (5)$$

$$\gamma_1 = \cos \frac{\theta_M}{2} e^{-i\phi_M}, \quad \gamma_2 = \sin \frac{\theta_M}{2} e^{i\phi_M} \quad (6)$$

where,  $\hat{U}$  is the operator which diagonalizes the  $\hat{H}(\mathbf{r})$ . The effective pair potential in the coordinate of spin space in ferromagnet is rewritten as

$$\hat{\Delta}^F(\theta_S) = \hat{U}^\dagger \hat{\Delta}(\theta_S) \hat{U}^* \quad (7)$$

Here, we consider the four types of pair potentials,  $d$ -wave,  $p_x$ -wave,  $p_y$ -wave and  $p_x + ip_y$ -wave. In  $d$ -wave case,

$$\Delta_{\uparrow\downarrow}(\theta_S) = -\Delta_{\downarrow\uparrow}(\theta_S) \equiv \Delta_0 f(\theta_S), \quad (8)$$

$$\Delta_{\uparrow\uparrow}(\theta_S) = \Delta_{\downarrow\downarrow}(\theta_S) = 0, \quad (9)$$

$$f(\theta_S) = \cos[2(\theta_S - \alpha)], \quad (10)$$

where  $\alpha$  is the angle between  $a$ -axis of the high- $T_c$  superconductor and the interface normal. The effective pair potential in the coordinate of spin space in ferromagnet is given by,

$$\begin{aligned} \hat{\Delta}^F(\theta_S) &\equiv \begin{pmatrix} \Delta_{\uparrow\uparrow}^F(\theta_S) & \Delta_{\uparrow\downarrow}^F(\theta_S) \\ \Delta_{\downarrow\uparrow}^F(\theta_S) & \Delta_{\downarrow\downarrow}^F(\theta_S) \end{pmatrix} \\ &= \begin{pmatrix} 0 & \Delta_0 \cos[2(\theta_S - \alpha)] \\ -\Delta_0 \cos[2(\theta_S - \alpha)] & 0 \end{pmatrix} \\ &= \hat{\Delta}(\theta_S). \end{aligned} \quad (11)$$

As shown in Eq. (11), the expression of the pair potential remains unchanged under the transformation in Eq.(4). Therefore transport properties are expected to be independent of the direction of the magnetic moment. This result can be applied to any singlet superconductors. On the other hand in spin-triplet superconductors, the pair potentials are given by

$$\Delta_{\uparrow\downarrow}(\theta_S) = \Delta_{\downarrow\uparrow}(\theta_S) = \Delta_0 f(\theta_S), \quad (12)$$

$$\Delta_{\uparrow\uparrow}(\theta_S) = \Delta_{\downarrow\downarrow}(\theta_S) = 0, \quad (13)$$

where the direction of the  $d$ -vector is parallel to the  $c$ -axis and

$$f(\theta_S) = \begin{cases} \cos \theta_S & \text{for } p_x - \text{symmetry}, \\ \sin \theta_S & \text{for } p_y - \text{symmetry}, \\ e^{i\theta_S} & \text{for } p_x + ip_y - \text{symmetry}. \end{cases} \quad (14)$$

Because the spin degree of freedom of Cooper pairs is active in triplet superconductors, the pair potential after the transformation in Eq.(4) depends on the direction of the magnetic moment

$$\hat{\Delta}^F(\theta_S) = \begin{pmatrix} \sin \theta_M & \cos \theta_M \\ \cos \theta_M & -\sin \theta_M \end{pmatrix} f(\theta_S) \Delta_0. \quad (15)$$

In general, there are four kinds of scattering processes with arbitrary  $H$  and  $\theta_M$  when an electron with majority spin is incident from ferromagnets:

- i) Andreev reflection to majority spin ( $a_{\uparrow\uparrow}$ )
- ii) Andreev reflection to minority spin ( $a_{\uparrow\downarrow}$ )
- iii) normal reflection to majority spin ( $b_{\uparrow\uparrow}$ ) and
- iv) normal reflection to minority spin ( $b_{\uparrow\downarrow}$ ).

Similar reflection processes also exist for the injection of an electron with minority-spin. Here,  $a_{\bar{s}\bar{s}'}$  and  $b_{\bar{s}\bar{s}'}$  are reflection coefficients of the Andreev and the normal reflections, respectively, where a quasiparticle is reflected from the spin-channel  $\bar{s}$  into the spin-channel  $\bar{s}'$ .

The wave function in ferromagnets for majority spin injection is represented by

$$\begin{aligned} \Psi_{\uparrow}(x) &= e^{ik_F \bar{\uparrow} x} \begin{pmatrix} 1 \\ 0 \\ 0 \\ 0 \end{pmatrix} + a_{\uparrow\uparrow} e^{ik_F \bar{\uparrow} x} \begin{pmatrix} 0 \\ 0 \\ 1 \\ 0 \end{pmatrix} + a_{\uparrow\downarrow} e^{ik_F \bar{\downarrow} x} \\ &\quad \times \begin{pmatrix} 0 \\ 0 \\ 0 \\ 1 \end{pmatrix} + b_{\bar{\uparrow}\bar{\uparrow}} e^{-ik_F \bar{\uparrow} x} \begin{pmatrix} 1 \\ 0 \\ 0 \\ 0 \end{pmatrix} + b_{\bar{\uparrow}\bar{\downarrow}} e^{-ik_F \bar{\downarrow} x} \begin{pmatrix} 0 \\ 1 \\ 0 \\ 0 \end{pmatrix} \end{aligned} \quad (16)$$

The wave function for minority spin injection is written in the similar way. In the above, we consider the situation  $k_{F\bar{\downarrow}} < k_S < k_{F\bar{\uparrow}}$ , where  $k_S \approx \sqrt{\frac{2mE_F}{\hbar^2}}$ . The coefficients  $a_{\bar{s}\bar{s}'}$  and  $b_{\bar{s}\bar{s}'}$  are determined by solving the BdG equation with quasiclassical approximation under appropriate boundary conditions.

The tunneling conductance  $\sigma_T(eV)$  for finite temperature is given by<sup>59,60,61</sup>

$$\sigma_T(eV) = \frac{2e^2}{h} G \quad (17)$$

$$\begin{aligned} G &= \frac{1}{16k_B T} \int_{-\infty}^{\infty} \int_{-\pi/2}^{\pi/2} d\theta_S \cos \theta_S dE \\ &\quad \times (\sigma_{S\bar{\uparrow}}(\theta_S) + \sigma_{S\bar{\downarrow}}(\theta_S)) \operatorname{sech}^2 \left( \frac{E - eV}{2k_B T} \right) \end{aligned} \quad (18)$$

$$\sigma_{S\bar{\uparrow}} = 1 + |a_{\bar{\uparrow}\bar{\uparrow}}|^2 - |b_{\bar{\uparrow}\bar{\uparrow}}|^2 + \left( \frac{\eta_{\bar{\downarrow}}}{\eta_{\bar{\uparrow}}} |a_{\bar{\uparrow}\bar{\downarrow}}|^2 - \frac{\eta_{\bar{\downarrow}}}{\eta_{\bar{\uparrow}}} |b_{\bar{\uparrow}\bar{\downarrow}}|^2 \right) \Theta(\theta_C - |\theta_S|) \quad \text{and}$$

$$\sigma_{S\bar{\downarrow}} = \left( 1 + \frac{\eta_{\bar{\uparrow}}}{\eta_{\bar{\downarrow}}} |a_{\bar{\downarrow}\bar{\uparrow}}|^2 + |a_{\bar{\downarrow}\bar{\downarrow}}|^2 - \frac{\eta_{\bar{\uparrow}}}{\eta_{\bar{\downarrow}}} |b_{\bar{\downarrow}\bar{\uparrow}}|^2 - |b_{\bar{\downarrow}\bar{\downarrow}}|^2 \right)$$

$$\times \Theta(\theta_C - |\theta_S|) \quad (19)$$

with  $Z_{\theta_S} = Z / \cos \theta_S$ ,  $Z = 2mH/\hbar^2 k_F$  and  $\eta_{\bar{\uparrow}(\bar{\downarrow})} = \sqrt{1 \pm X / \cos^2 \theta_S}$ . Here, we define the polarization parameter by  $X = U/E_F$ . The quantity  $\sigma_{S\bar{\uparrow}(\bar{\downarrow})}$  is the tunneling conductance for an incident electron with the majority (minority) spin. For  $|\theta_S| > \theta_C = \cos^{-1} \sqrt{X}$ , the reflected wave becomes an evanescent wave and does not contribute to the tunneling conductance. As seen from above equations, the tunneling conductance depends on  $\theta_M$  only when superconductors have spin-triplet Cooper pairs. The tunneling conductance  $\Gamma$  can be summarized in a following simple equation in a several cases:

$$\sigma_{S\bar{\uparrow}} = \sigma_{N\bar{\uparrow}}(A + B), \quad (20)$$

$$\sigma_{S\bar{\downarrow}} = \sigma_{N\bar{\downarrow}}C \quad (21)$$

$$A = \frac{\Theta(\theta_C - |\theta_S|)[1 - |\Gamma_+ \Gamma_-|^2(1 - \sigma_{N\bar{\uparrow}}) + \sigma_{N\bar{\downarrow}}|\Gamma_+|^2]}{|1 - \Gamma_+ \Gamma_- \sqrt{1 - \sigma_{N\bar{\downarrow}}} \sqrt{1 - \sigma_{N\bar{\uparrow}}} \exp[i(\varphi_{\bar{\downarrow}} - \varphi_{\bar{\uparrow}})]|^2} \quad (22)$$

$$B = \frac{[1 - \Theta(\theta_C - |\theta_S|)][1 - |\Gamma_+ \Gamma_-|^2]}{1 - \Gamma_+ \Gamma_- \sqrt{1 - \sigma_{N\bar{\downarrow}}} \exp[i(\varphi_{\bar{\downarrow}} - \varphi_{\bar{\uparrow}})]}, \quad (23)$$

$$C = \frac{\Theta(\theta_C - |\theta_S|)[1 - |\Gamma_+ \Gamma_-|^2(1 - \sigma_{N\bar{\uparrow}}) + \sigma_{N\bar{\uparrow}}|\Gamma_+|^2]}{|1 - \Gamma_+ \Gamma_- \sqrt{1 - \sigma_{N\bar{\downarrow}}} \sqrt{1 - \sigma_{N\bar{\uparrow}}} \exp[i(\varphi_{\bar{\uparrow}} - \varphi_{\bar{\downarrow}})]|^2} \quad (24)$$

with

$$\exp(i\varphi_{\bar{\downarrow}}) = \frac{1 - \eta_{\bar{\downarrow}} + iZ_{\theta_S}}{\sqrt{1 - \sigma_{N\bar{\downarrow}}}(1 + \eta_{\bar{\downarrow}} - iZ_{\theta_S})}, \quad (25)$$

$$\exp(-i\varphi_{\bar{\uparrow}}) = \frac{1 - \eta_{\bar{\uparrow}} - iZ_{\theta_S}}{\sqrt{1 - \sigma_{N\bar{\uparrow}}}(1 + \eta_{\bar{\uparrow}} - iZ_{\theta_S})}, \quad (26)$$

when superconductors have the spin-singlet Cooper pairs and  $\theta_M$  is 0 or  $\pi$  in triplet superconductors. When  $\theta_M = \pi/2$  in triplet superconductors,

$$\sigma_{S\bar{\uparrow}} = \sigma_{N\bar{\uparrow}} \frac{1 - |\Gamma_+ \Gamma_-|^2(1 - \sigma_{N\bar{\uparrow}}) + \sigma_{N\bar{\uparrow}}|\Gamma_+|^2}{|1 - \Gamma_+ \Gamma_- (1 - \sigma_{N\bar{\uparrow}})|^2} \quad (27)$$

$$\sigma_{S\bar{\downarrow}} = \sigma_{N\bar{\downarrow}} \frac{1 - |\Gamma_+ \Gamma_-|^2(1 - \sigma_{N\bar{\downarrow}}) + \sigma_{N\bar{\downarrow}}|\Gamma_-|^2}{|1 - \Gamma_+ \Gamma_- (1 - \sigma_{N\bar{\downarrow}})|^2} \times \Theta(\theta_C - |\theta_S|). \quad (28)$$

Here,  $\Gamma_{\pm}$  is defined as

$$\Gamma_{\pm} = \pm \frac{E - \sqrt{E^2 - |\Delta(\theta_S)|^2}}{\Delta(\theta_S)^*}, \quad (29)$$

$$\sigma_{N\bar{\uparrow}} = \frac{4\eta_{\bar{\uparrow}}}{(1 + \eta_{\bar{\uparrow}})^2 + Z_{\theta_S}^2} \quad (30)$$

$$\sigma_{N\bar{\downarrow}} = \frac{4\eta_{\bar{\downarrow}}}{(1 + \eta_{\bar{\downarrow}})^2 + Z_{\theta_S}^2} \Theta(\theta_C - |\theta_S|) \quad (31)$$

We describe the dependence of the pair potential on temperatures by solving the BCS's gap equation.

In general, the pair potential deviates from step function near the interface. The spatial dependence of the pair potential can be described by  $\bar{\Delta}(\theta_S, x)$  with  $\bar{\Delta}(\theta_S, x) = \bar{\Delta}(\theta_S, x)\Theta(x)$ .

In order to determine the spatial dependence of  $\bar{\Delta}(\theta_S, x)$ , we apply quasi-classical Green's function theory developed by Hara, Nagai, *et al.*<sup>2,56,62,63</sup>. In the following, we will explain in the case of singlet pairing. Extension to triplet case for the present *p*-wave cases is straightforward. The spatial dependence of  $\bar{\Delta}(\theta_S, x)$  is calculated by the diagonal elements of matrix green function in directional space. The diagonal matrix element of the quasi-classical Green's function  $g_{\alpha\alpha}(x)$  is reproduced by the quantity  $D_{\alpha}(x)$  and  $F_{\alpha}(x)$ ,

$$g_{++}(\theta_S, x) = i \begin{pmatrix} \frac{1+D_+(x)F_+(x)}{1-D_+(x)F_+(x)} & \frac{2iF_+(x)}{1+D_+(x)F_+(x)} \\ \frac{2iD_+(x)}{1-D_+(x)F_+(x)} & -\frac{1+D_+(x)F_+(x)}{1-D_+(x)F_+(x)} \end{pmatrix}, \quad (32)$$

$$g_{--}(\theta_S, x) = i \begin{pmatrix} \frac{1+D_-(x)F_-(x)}{-1+D_-(x)F_-(x)} & \frac{2iF_-(x)}{-1+D_-(x)F_-(x)} \\ \frac{2iD_-(x)}{-1+D_-(x)F_-(x)} & -\frac{1+D_-(x)F_-(x)}{-1+D_-(x)F_-(x)} \end{pmatrix} \quad (33)$$

with direction index  $\alpha = \pm$  which specifies the momentum direction along the  $x$  axis. The functions  $D_{\alpha}(x)$  and  $F_{\alpha}(x)$  obey the following equations

$$\hbar|v_{Fx}|D_{\alpha}(x)$$

$$= \alpha [2\omega_m D_{\alpha}(x) + \bar{\Delta}(\theta_S, x)D_{\alpha}^2(x) - \bar{\Delta}^*(\theta_S, x)] \quad (34)$$

$$\hbar|v_{Fx}|F_{\alpha}(x)$$

$$= \alpha [-2\omega_m F_{\alpha}(x) + \bar{\Delta}^*(\theta_S, x)F_{\alpha}^2(x) - \bar{\Delta}(\theta_S, x)]. \quad (35)$$

$$\bar{\Delta}(\theta_S, x) = \begin{pmatrix} 0 & \bar{\Delta}(\theta_S, x) \\ -\bar{\Delta}(\theta_S, x) & 0 \end{pmatrix} \quad (36)$$

The boundary conditions at the interface are given by<sup>64,65</sup>

$$F_+(0) = \frac{(\eta_{\bar{\uparrow}} - 1 + iZ)(\eta_{\bar{\downarrow}} - 1 - iZ)}{(\eta_{\bar{\uparrow}} + 1 + iZ)(\eta_{\bar{\downarrow}} + 1 - iZ)} D_-(0)^{-1} \quad (37)$$

$$F_-^{-1}(0) = \frac{(\eta_{\bar{\uparrow}} - 1 + iZ)(\eta_{\bar{\downarrow}} - 1 - iZ)}{(\eta_{\bar{\uparrow}} + 1 + iZ)(\eta_{\bar{\downarrow}} + 1 - iZ)} D_+(0). \quad (38)$$

We first solve  $D_{\pm}(x)$ ,  $F_{\pm}(x)$  and calculate  $g_{\pm,\pm}(\theta, x)$  for given  $\bar{\Delta}(\theta_S, x)$ . By using  $g_{\pm,\pm}(\theta, x)$ ,  $\bar{\Delta}(\theta_S, x)$  is recalculated as follows

$$\check{\Delta}(\theta_S, x) = \sum_{n\alpha} \int_{\pi/2}^{\pi/2} d\theta_{S'} V(\theta_S, \theta'_S) g_{\alpha,\alpha}(\theta'_S, x) \quad (39)$$

with  $V(\theta, \theta') = g_0 f(\theta) f(\theta')$ , where

$$g_0 = \frac{2\pi k_B T}{\ln(T/T_C) + \sum_{0 < m < m_a} \frac{1}{m+1/2}} \quad (40)$$

with cutoff value  $m_a$  and  $f(\theta)$  is given in Eqs. (10) and (14). The iteration is carried out until the sufficient convergence is obtained. We finally obtain  $\bar{\Delta}(\theta, x)$ , i.e.,  $\hat{\Delta}(\theta, x)$ . Using this self-consistently determined pair potentials, we obtain  $\check{\Gamma}_{\pm}(x)$  by solving

$$i\hbar|v_{Fx}|\check{\Gamma}_{+}(x) = \alpha [2E\check{\Gamma}_{+}(x) - \bar{\Delta}(\theta_S, x)\check{\Gamma}_{+}^2(x) - \bar{\Delta}^*(\theta_S, x)], \quad (41)$$

$$i\hbar|v_{Fx}|\check{\Gamma}_{-}(x) = \alpha [2E\check{\Gamma}_{-}(x) - \bar{\Delta}^*(\theta_S, x)\check{\Gamma}_{-}^2(x) - \bar{\Delta}(\theta_S, x)] \quad (42)$$

By substituting  $\Gamma_{\pm}$  into Eqs. (20)-(29) with  $\check{\Gamma}(x = 0)$ , tunneling conductance is obtained. In the following section, we assume that the transition temperature of Ferromagnet is much larger than  $T_C$  which is the transition temperature of superconductor. Then we can neglect the temperature dependence of  $X$ .

### III. RESULTS

#### A. polarization dependence of zero-bias conductance

In this subsection, we calculate the ZBC as a function of the spin-polarization in ferromagnets ( $X$ ) at zero temperature. The dimensionless ZBC ( $\Gamma$ ) is given by

$$\Gamma = \frac{\sigma_T(0)h}{2e^2} \quad (43)$$

At first we show results obtained in the step-function model, where spatial dependence of the pair potential is not determined self-consistently (non-SCF calculation).  $X$ -dependence of  $\Gamma$  at the zero temperature for  $d$ -wave junctions is plotted in Fig. 2. The magnitude of  $\Gamma$  is always a decreasing function of  $X$ . For  $\alpha = 0$  (Fig. 2(a)),  $\Gamma$  decreases with increasing of  $Z$ . On the other hand, for  $\alpha = \pi/4$  (Fig. 2(b)),  $\Gamma$  is completely independent of  $Z$  since the perfect Andreev reflection occurs due to the formation of the zero energy resonance state at the interface.

Next, we show the polarization dependence of  $\Gamma$  for triplet  $p_x$ ,  $p_y$  and  $p_x + ip_y$ -wave superconductors, where the pair potential are given in Eqs. (12), (13) and (14). The polarization dependence of  $\Gamma$  for  $p_x$ ,  $p_y$  and  $p_x + ip_y$

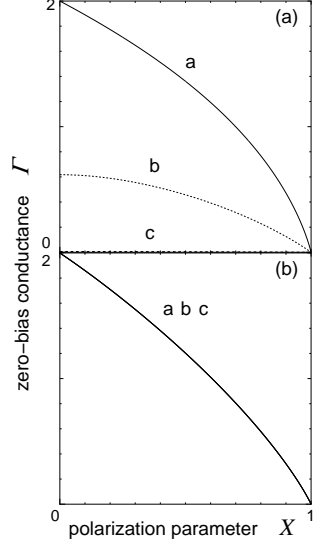


FIG. 2:  $X$  dependence of the zero-bias conductance  $\Gamma$  in non-SCF calculation for (a)  $\alpha = 0$  and (b)  $\alpha = \pi/4$  for  $d$ -wave junctions at zero temperature. a:  $Z = 0$ , b:  $Z = 1$  and c:  $Z = 5$ .

wave junctions are shown in Fig. 3. As shown in Fig. 3,  $\Gamma$  changes drastically by  $\theta_M$  which is a property peculiar to  $p$ -wave junctions. For  $\theta_M = 0$ , as shown in Figs. 3 (a), (d), and (g)  $\Gamma$  approaches to zero in the limit of  $X \rightarrow 1$  independent of the magnitude of  $Z$ . In these cases, the diagonal elements in Eq. (3) disappear and a quasiparticle suffers the spin-flip in the Andreev reflection, (i.e.,  $a_{\uparrow,\uparrow} = a_{\downarrow,\downarrow} = 0$ ). For  $|\theta_S| > \theta_C$ , the Andreev reflection to  $\downarrow$  spin becomes the evanescent wave and incident wave with  $\downarrow$  spin vanishes. Then the magnitude of  $\Gamma$  vanishes in the limit of  $X = 1$ , where ferromagnets are referred to as half-metals. On the other hand, for  $\sin\theta_M \neq 0$ ,  $\Gamma$  take finite values even in  $X \rightarrow 1$  as shown in Figs. 3 (b) (c), (e) (f) (h), and (i) because the spin-conserved Andreev reflection is still possible in these junctions. When  $\theta_M = \pi/2$ , results for which are shown in Figs. 3 (b) (e) and (h) the off-diagonal elements in Eq. (15) become zero. Thus spin of a quasiparticle is conserved in the Andreev reflection, (i.e.,  $a_{\uparrow,\downarrow} = a_{\downarrow,\uparrow} = 0$ ). The Andreev reflection of an electron with  $\uparrow$  spin survives irrespective of  $\theta_S$ , whereas that of an electron with  $\downarrow$  spin vanishes for  $|\theta_S| > \theta_C$ . We note in  $p_x$ -wave junctions that  $\Gamma$  does not depend on  $Z$  as well as  $d$ -wave junctions with  $\alpha = \pi/4$ . This is because the ZES's are formed at the interface.

Secondly, we calculate the tunneling conductance under the pair potential whose spatial dependence is determined self-consistently (SCF calculation). The results for  $d$ ,  $p_x$ ,  $p_y$ , and  $p_x + ip_y$ -wave junctions are shown in Figs. 4 and 5 respectively. The conductance in SCF calculation in Figs. 4 and 5 should be compared with corresponding results in non-SCF calculation in Figs. 2 and 3, respectively. We do not find any remarkable differences between the results in SCF calculation and those

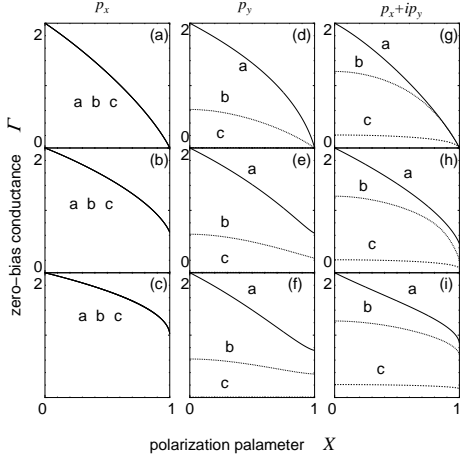


FIG. 3:  $X$  dependence of  $\Gamma$  in non-SCF calculation. (a)  $\theta_M = 0$ , (b)  $\theta_M = \pi/4$  and (c)  $\theta_M = \pi/2$  for  $p_x$ -wave junctions. (d)  $\theta_M = 0$ , (e)  $\theta_M = \pi/4$  and (f)  $\theta_M = \pi/2$  for  $p_y$ -wave junctions. (g)  $\theta_M = 0$ , (h)  $\theta_M = \pi/4$  and (i)  $\theta_M = \pi/2$  for  $p_x + ip_y$ -wave junctions. a:  $Z = 0$ , b:  $Z = 1$  and c:  $Z = 5$ .

in non-SCF calculation as shown in these figures.

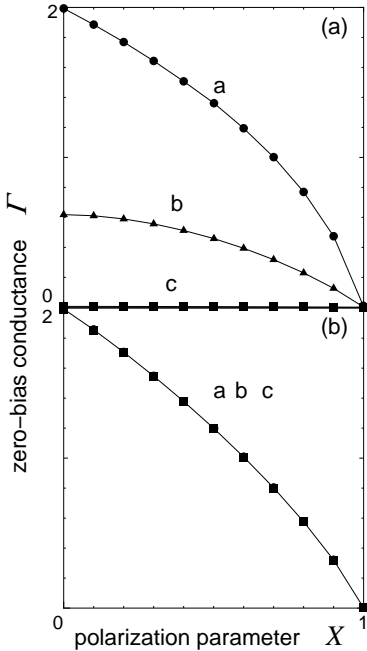


FIG. 4:  $X$  dependence of  $\Gamma$  in SCF calculation for  $d$ -wave junctions. (a)  $\alpha = 0$  and (b)  $\alpha = \pi/4$ . a:  $Z = 0$ , b:  $Z = 1$  and c:  $Z = 5$ .

### B. Temperature dependence of zero-bias conductance

In this subsection, we show the temperature dependence of  $\Gamma$ . In the first part, we discuss the conductance

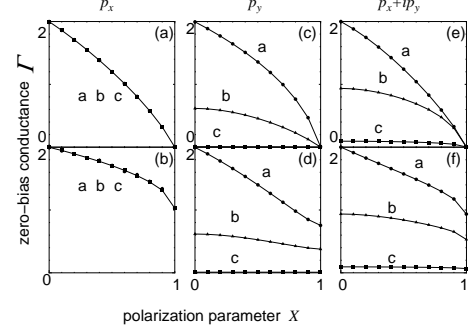


FIG. 5:  $X$  dependence of  $\Gamma$  in SCF calculation. (a)  $\theta_M = 0$  and (b)  $\theta_M = \pi/2$  with  $p_x$ -wave junctions. (c)  $\theta_M = 0$  and (d)  $\theta_M = \pi/2$  with  $p_y$ -wave junctions. (e)  $\theta_M = 0$  and (f)  $\theta_M = \pi/2$  with  $p_x + ip_y$ -wave junctions. a:  $Z = 0$ , b:  $Z = 1$  and c:  $Z = 5$ .

in the non-SCF calculation. Then the results are compared with those in the SCF calculation in the second part. First let us focus on  $d$ -wave junctions for  $\alpha = 0$  as shown in Figs. 6 (a), (b), (c), where the conductance is plotted as a function of temperatures for several magnitudes of the exchange potential  $X$ . We note in these junctions that the ZES is not formed at the interface. For  $Z = 0$  (see Fig. 6(a)), the exchange potential in ferromagnets significantly affects the temperature-dependence of  $\Gamma$ . For the large magnitudes of  $X$ ,  $\Gamma$  increases with the increase of  $T$  as shown in the curve  $d$  of Fig. 6(a). The Andreev reflection (two-electron process) is suppressed by the large exchange potential and the current is mainly carried by single electron process. While for small magnitudes of  $X$ ,  $\Gamma$  decreases with the increase of  $T$  as shown in curve  $a$  in Fig. 6(a). This is because the current at the zero-voltage is mainly carried by two-electron process thorough the Andreev reflection and the amplitude of the Andreev reflection is suppressed for  $T \rightarrow T_C$ . For  $Z = 5$  (Fig. 6(c)), the height of  $\Gamma$  becomes small around  $T \sim 0$  because the insulating barrier suppresses the Andreev reflection. The results show that  $\Gamma$  increases monotonically with increasing temperatures independent of the magnitudes of  $X$  since the current is mainly carried by single electron process. For  $Z = 1$  (Fig. 6(b)), except for large magnitude of  $X$ , the magnitude of  $\Gamma$  has a non-monotonous temperature-dependence, since the amplitude of single-electron process (Andreev reflection) is enhanced (suppressed) with the increase of  $T$ .

We calculate the temperature-dependence of  $\Gamma$  in  $d$ -wave junctions with  $\alpha = \pi/4$  as shown in Figs. 6(d), (e), and (f). In these junctions, the ZES is formed at the interface and dominates transport properties for sufficiently large  $Z$ . For  $Z = 0$ , the line shape of the all curves in Fig. 6(d) are qualitatively similar to those with  $\alpha = 0$  shown in Fig. 6(a) since ZES is not formed at the interface. We note in Fig. 11 that  $\Gamma$  at the zero temperature is independent of  $Z$  as shown in  $Z = 1$  (Fig. 6(e)) and  $Z = 5$  (Fig. 6(f)). This is because the perfect An-

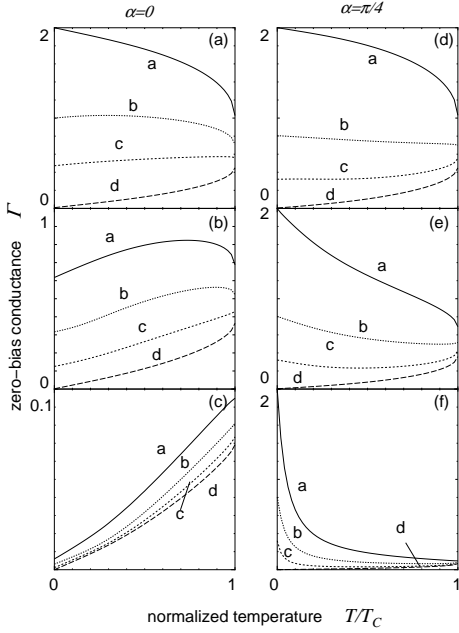


FIG. 6: Temperature dependence of  $\Gamma$  in non-SCF calculation for  $d$ -wave junctions. (a)  $Z = 0$ , (b)  $Z = 1$  and (c)  $Z = 5$  with  $\alpha = 0$ . (d)  $Z = 0$ , (e)  $Z = 1$  and (f)  $Z = 5$  with  $\alpha = \pi/4$ . a:  $X = 0$ , b:  $X = 0.7$ , c:  $X = 0.9$  and d:  $X = 0.999$ .

Andreev reflection occurs due to the formation of the ZES at the interface. The feature of the resonant tunneling becomes prominent for the larger magnitude of  $Z$ , and the amplitude of  $\Gamma$  is proportional to the inverse of  $T$  for intermediate temperature region (curve a in Fig. 6(f)). Since the retro-reflectivity of Andreev reflection is broken at finite exchange potentials, the degree of resonance at the interface is weakened and the temperature-dependence deviates from the inverse of  $T$ . For sufficiently large magnitudes of  $X$ ,  $\Gamma$  is no more a decreasing function of  $T$  but an increasing function of  $T$  as in the case of Fig. 6(f). Through the temperature-dependence of  $\Gamma$ , we can estimate the order of the magnitude of  $X$ .

Next, we discuss temperature-dependence of  $\Gamma$  in  $p_x$ -wave junctions with  $\theta_M = 0$  (Figs. 7(a), (b), (c)) and  $\pi/2$  (Figs. 8(a), (b), (c)), in  $p_y$ -wave junctions with  $\theta_M = 0$  (Figs. 7(d), (e), (f)) and  $\pi/2$  (Figs. 8(d), (e), (f)), and in  $p_x + ip_y$ -wave junctions with  $\theta_M = 0$  (Figs. 7(g), (h), (i)) and  $\pi/2$  (Figs. 8(g), (h), (i)). As shown in Figs. 7(a), (b), (c), the temperature dependence of  $\Gamma$  is quite similar to that of  $d$ -wave junctions with  $\alpha = \pi/4$ . In  $p_x$ -wave junctions with  $\theta_M = 0$ ,  $\Gamma$  with small  $X$  are decreasing function of  $T$ , whereas  $\Gamma$  with large  $X$  is increasing function of  $T$ . In  $p_x$ -wave junctions with  $\theta_M = \pi/2$ , however, all  $\Gamma$  becomes monotonically decreasing function of  $T$  (see Figs. 8(a), (b), (c)) independent of  $Z$ . In the case of  $\theta_M = \pi/2$ , the spin of a quasiparticle is always conserved in the Andreev reflection. In the case of  $\theta_M = \pi/2$ , the spin of a quasiparticle is conserved in the Andreev reflection, therefore, the suppression of conductance due to the

breakdown of retro-reflectivity becomes weaker than that in the case of  $\theta_M = 0$ .

In  $p_y$ -wave junctions with  $\theta_M = 0$ , temperature-dependence of  $\Gamma$  shown in Figs. 7(d), (e), (f) are similar to those of  $d$ -wave junctions with  $\alpha = 0$  shown in Figs. 6(a), (b), (c), where no ZES is expected in both cases. In  $p_y$ -wave junctions with  $\theta_M = \pi/2$  as shown in Figs. 8(d), (e), (f),  $\Gamma$  for large  $X$  are larger than those with  $\theta_M = 0$  in low temperatures with  $Z=0$  and 5. In the case of  $\theta_M = \pi/2$ , the spin of a quasiparticle is conserved in the Andreev reflection, therefore, the suppression of conductance due to the breakdown of retro-reflectivity becomes weaker than that in the case of  $\theta_M = 0$ .

In  $p_x + ip_y$ -wave junctions with  $\theta_M = 0$ , temperature-dependence of  $\Gamma$  can be understood by the interpolation of the results in  $p_x$ -wave and  $p_y$ -wave junctions because the ZES is only expected for a quasiparticle with perpendicular injection to the interface<sup>37</sup>. As seen from Fig. 7(g) for  $Z=0$ , there is no clear difference between  $\Gamma$  in  $p_x + ip_y$ -wave junctions with  $\theta_M = 0$  and corresponding results in  $p_x$  or  $p_y$ -wave junctions shown in Figs. 7(a) and (d). For a finite barrier potential at  $Z = 1$ , the line shape of the all curves in Fig. 7(h) is rather similar to corresponding results in the  $p_x$ -wave junctions than those in the  $p_y$ -wave junctions. However, the amplitudes of  $\Gamma$  are smaller than those in the  $p_x$ -wave junctions. For  $Z = 5$ , the magnitude of  $\Gamma$  is enhanced at low temperature with small  $X$ , due to the formation of ZES with perpendicular injection [see curve a in Fig. 7(i)]. On the other hand, for large magnitude of  $X$ ,  $\Gamma$  is an increasing function of  $T$  [see curve d in Fig. 7(i)]. For  $\theta_M = \pi/2$ ,  $\Gamma$  becomes a decreasing function of  $T$  for every case as seen from Figs. 8(g), (h), (i) similar to the  $p_x$ -wave case.

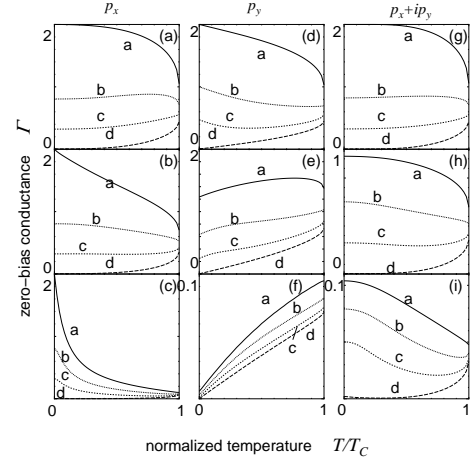


FIG. 7: Temperature dependence of  $\Gamma$  in non-SCF calculation for  $\theta_M = 0$ . (a)  $Z = 0$ , (b)  $Z = 1$  and (c)  $Z = 5$  in  $p_x$ -wave junctions. (d)  $Z = 0$ , (e)  $Z = 1$  and (f)  $Z = 5$  in  $p_y$ -wave junctions. (g)  $Z = 0$ , (h)  $Z = 1$  and (i)  $Z = 5$  in  $p_x + ip_y$ -wave junctions. a:  $X = 0$ , b:  $X = 0.7$ , c:  $X = 0.9$  and d:  $X = 0.999$ .

It is important to check how the above results are modified in the presence of the spatial dependence in the pair

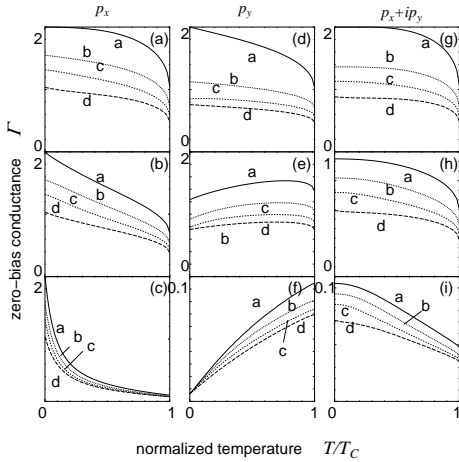


FIG. 8: Temperature dependence of  $\Gamma$  in non-SCF calculation for  $\theta_M = \pi/2$ . (a)  $Z = 0$ , (b)  $Z = 1$  and (c)  $Z = 5$  in  $p_x$ -wave junctions. (d)  $Z = 0$ , (e)  $Z = 1$  and (f)  $Z = 5$  in  $p_y$ -wave junctions. (g)  $Z = 0$ , (h)  $Z = 1$  and (i)  $Z = 5$  in  $p_x+ip_y$ -wave junctions. a:  $X = 0$ , b:  $X = 0.7$ , c:  $X = 0.9$  and d:  $X = 0.999$ .

potential near the interface. In what follows, we consider two limits of  $X$ , i.e., small limit of the exchange potential  $X = 0$  (curve a) and large limit of  $X = 0.9$  (curve b). The corresponding results in non-SCF calculation are curves a ( $X=0$ ) and c ( $X=0.9$ ) from Figs. 6 to 8. In Fig. 9, we show the conductance in SCF calculation in the  $d$ -wave junctions with  $\alpha = 0$  and  $\pi/4$ , respectively. For  $d$ -wave junctions, temperature-dependence of  $\Gamma$  with  $\alpha = 0$  obtained in SCF calculation is quite similar to that in non-SCF way when we compare Figs. 6(a), (b), (c) and 9(a), (b), (c). The same tendency can be seen in the  $d$ -wave junctions with  $\alpha = \pi/4$  as shown in Figs. 6 (d), (e), (f) and 9(d), (e), (f). Although the spatial depletion of the pair potential near the interface is significant for  $Z = 5$ ,  $\Gamma$  is still a decreasing function of  $T$ . This characteristic feature is considered to be insensitive to the profile of the pair potential because it is a consequence of the formation of the ZES which stems from the sign-change of the pair potential.

In the  $p_x$ -wave junctions, line shapes of  $\Gamma$  for  $\theta_M = 0$  shown in Figs. 10(a), (b), (c) are quite similar to those in the  $d$ -wave junctions with  $\alpha = \pi/4$ . For  $\theta_M = \pi/2$ , as shown in Figs. 11(a), (b), (d), the magnitudes of  $\Gamma$  are slightly larger than those in Figs. 10(a), (b), (c). These features are almost similar to those found in non-SCF calculation in Figs. 7(a), (b), (c) and 8(a), (b), (c).

As well as in the  $p_x$ -wave junctions, the characteristic behavior of  $\Gamma$  in SCF results in  $p_y$ -wave junctions shown in Figs. 10(d), (e), (f) and 11(d), (e), (f) are almost the same with those obtained in non-SCF calculation shown in Figs. 7(d), (e), (f) and 8(d), (e), (f).

In the case of  $p_x+ip_y$ -wave symmetry, the line-shape of  $\Gamma$  for (g), (h) and (i) in Figs. 10 and 11 are similar to those in non SCF results shown in (g) and (h) in Figs. 7 and

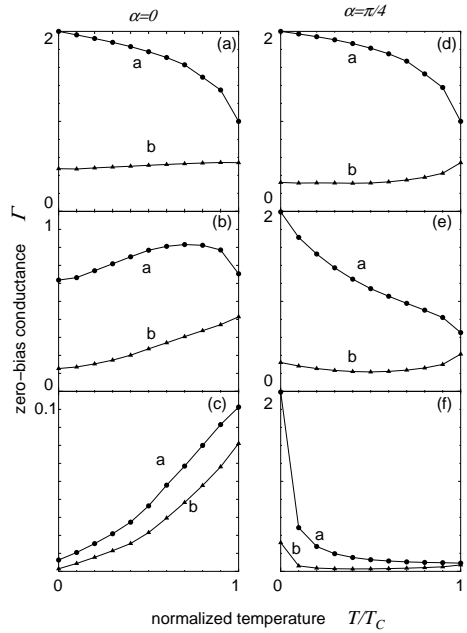


FIG. 9: Temperature dependence of  $\Gamma$  in SCF calculation for  $d$ -wave junctions. (a)  $Z = 0$ , (b)  $Z = 1$  and (c)  $Z = 5$  with  $\alpha = 0$ . (d)  $Z = 0$ , (e)  $Z = 1$  and (f)  $Z = 5$  for  $\alpha = \pi/4$ . a:  $X = 0$  and b:  $X = 0.9$ .

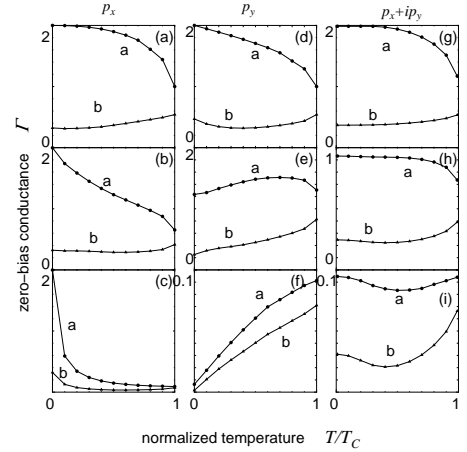


FIG. 10: Temperature dependence of  $\Gamma$  in SCF calculation for  $\theta_M = 0$ . (a)  $Z = 0$ , (b)  $Z = 1$  and (c)  $Z = 5$  in  $p_x$ -wave junctions. (d)  $Z = 0$ , (e)  $Z = 1$  and (f)  $Z = 5$  in  $p_y$ -wave junctions. (g)  $Z = 0$ , (h)  $Z = 1$  and (i)  $Z = 5$  in  $p_x+ip_y$ -wave junctions. a:  $X = 0$  and b:  $X = 0.9$ .

8. However, the temperature-dependencies of  $\Gamma$  based on SCF calculation deviate from those on non SCF one for large  $Z$  [Fig. 10(i) and Fig. 11(i)]. In SCF calculation,  $\Gamma$  first decreases with the increase of  $T$  then increases. The decreasing temperature dependence is similar to  $p_x$ -wave case due to the ZES and increasing one is similar to  $p_y$ -wave case. In this case, since only the quasiparticle injected perpendicular to the interface contribute to the

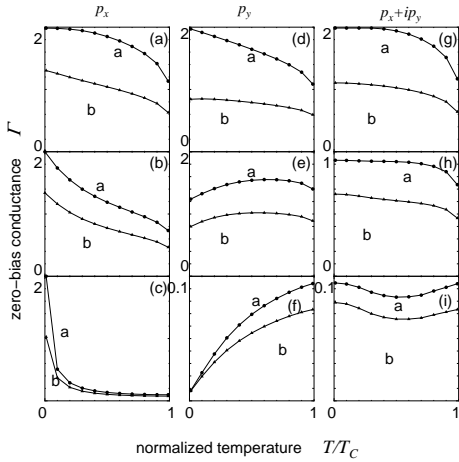


FIG. 11: Temperature dependence of  $\Gamma$  in non-SCF calculation for  $\theta_M = \pi/2$ . (a)  $Z = 0$ , (b)  $Z = 1$  and (c)  $Z = 5$  in  $p_x$ -wave junctions. (d)  $Z = 0$ , (e)  $Z = 1$  and (f)  $Z = 5$  in  $p_y$ -wave junctions. (g)  $Z = 0$ , (h)  $Z = 1$  and (i)  $Z = 5$  in  $p_x + ip_y$ -wave junctions. a:  $X = 0$  and b:  $X = 0.9$ .

ZES and the resulting ZBC is sensitive to the spatial dependence of the pair potentials<sup>28</sup>.

#### IV. SUMMARY

In this paper, we have calculated the polarization and temperature dependence of the zero-bias conductance (ZBC) in  $F/I/S$  junctions, where we have chosen the symmetry of the pair potential as  $d$ -wave for high  $T_C$  cuprate and  $p_x + ip_y$  for  $\text{Sr}_2\text{RuO}_4$ . As a reference, we have also studied  $p_x$  and  $p_y$ -wave junctions. We have made a formalism of ZBC which is available for the arbitrary angle  $\theta_M$ , the angle between the magnetization axis of the ferromagnet and  $c$ -axis of the superconductor. The  $\theta_M$  dependence of the tunneling conductance only appears for triplet superconductor cases. We have clarified following points.

(1) When injected quasiparticles from ferromagnet always feel zero energy resonance state, *e.g.*,  $d$ -wave junction with (110) orientation and  $p_x$ -wave junction, zero bias

tunneling conductance (ZBC) at zero temperature is insensitive to the barrier potential at the interface. This property is useful for the determination of the magnitude of polarization of ferromagnet at sufficiently low temperatures.

(2) For  $d$ -wave junctions with (110) orientation and  $p_x$ -wave junctions, ZBC is a decreasing function with temperature when the degree of the polarization,  $X$ , is small. On the other hand, for large magnitude of  $X$ , ZBC is an increasing function of  $T$ . While for  $d$ -wave junctions with (100) orientation and  $p_y$ -wave junctions, where ZES does not appear, ZBC is an increasing function of  $T$  independent of  $X$ . For  $p_x + ip_y$ -wave junctions, ZBC first decreases and increases again.

(3) For  $p$ -wave junctions, ZBC has different temperature dependence depending on the direction of the magnetization axis of ferromagnet. This unique property is peculiar to triplet pairing.

(4) Throughout this paper, we have calculated ZBC both for two cases; i) spatial dependence of the pair potential is assumed to be step function (non-SCF calculation) ii) spatial depletion of the pair potentials are determined self-consistently (SCF-calculation). We have clarified that obtained results based on non-SCF calculation is almost similar to those for SCF-calculation.

In this paper, the effect of random potential in ferromagnet is not taken into account. Recently, there are several works about random scattering effect in unconventional superconductor junctions<sup>66,67,68,69</sup>. It is actually interesting problem to study about the influence of the diffusive scattering in ferromagnet on the ZBC. In the present paper, the splitting of ZBCP by magnetic field due to Zeeman effect or magnetic impurity in the insulator is not taken into account<sup>40,41,42</sup>. It is also an interesting future problem.

#### Acknowledgments

This work was partially supported by the Core Research for Evolutional Science and Technology (CREST) of the Japan Science and Technology Corporation (JST). J.I. acknowledges support by the NEDO international Joint Research project "Nano-scale Magnetoelectronics".

<sup>1</sup> L. J. Buchholtz and G. Zwicknagl, Phys. Rev. B **23**, 5788 (1981).

<sup>2</sup> J. Hara and K. Nagai, Prog. Theor. Phys. **76**, 1237 (1986).

<sup>3</sup> C. R. Hu, Phys. Rev. Lett. **72**, 1526 (1994).

<sup>4</sup> S. Kashiwaya, Y. Tanaka, M. Koyanagi, and K. Kajimura, Phys. Rev. B **51**, 1350 (1995).

<sup>5</sup> L. Alff, H. Takashima, S. Kashiwaya, N. Terada, Y. Tanaka, M. Koyanagi and K. Kajimura, Phys. Rev. B **55** (1997) 14757.

<sup>6</sup> M. Covington, M. Aprili, E. Paraoanu, L.H. Greene, F. Xu, J. Zhu and C.A. Mirkin, Phys. Rev. Lett. **79**, 277 (1997).

<sup>7</sup> J. Y. T. Wei, N.-C. Yeh, D. F. Garrigus, and M. Strasik, Phys. Rev. Lett. **81**, 2452 (1998).

<sup>8</sup> W. Wang, M. Yamazaki, K. Lee, and I. Iguchi, Phys. Rev. B **60**, 4272 (1999).

<sup>9</sup> I. Iguchi, W. Wang, M. Yamazaki, Y. Tanaka and S. Kashiwaya, Phys. Rev. B **62**, R6131 (2000).

<sup>10</sup> Y. Tanaka and S. Kashiwaya, Phys. Rev. B **53**, 9371 (1996).

<sup>11</sup> Y. Tanaka and S. Kashiwaya, Phys. Rev. B **53**, 11957 (1996); **56**, 892 (1997); **58**, 2948 (1998).

<sup>12</sup> Y. Tanaka and S. Kashiwaya, J. Phys. Soc. Jpn. **68**, 3485

(1999); **69**, 1152 (2000).

<sup>13</sup> Y. Asano, Phys. Rev. B **63**, 052512 (2001).

<sup>14</sup> Y. Tanuma, Y. Tanaka, M. Yamashiro and S. Kashiwaya, Phys. Rev. B **58**, 7997 (1998).

<sup>15</sup> Y. Tanauma, Y. Tanaka, M. Ogata and S. Kashiwaya. J. Phys. Soc. Jpn., **67**, pp.1118-1121, (1998).

<sup>16</sup> Y. Tanuma, Y. Tanaka, M. Ogata and S. Kashiwaya, Phys. Rev. B **60**, 9817 (1999).

<sup>17</sup> Y. Tanaka, T. Asai, N. Yoshida, J. Inoue and S. Kashiwaya, Phys. Rev. B **61**, R11902, (2000).

<sup>18</sup> Y. Tanaka, Y. Tanuma and S. Kashiwaya, Phys. Rev. B, **64**, 054510, (2001).

<sup>19</sup> Y. Tanaka, H. Tsuchiura, Y. Tanuma and S. Kashiwaya, J. Phys. Soc. Jpn. **71** 271, (2002).

<sup>20</sup> Y. Tanaka, H. Itoh, H. Tsuchiura, Y. Tanuma, J. Inoue, J. Phys. Soc. Jpn., **71** 2005, (2002).

<sup>21</sup> S. Ryu and Y. Hatsugai, Phys. Rev. Lett. **89** 077002 (2002).

<sup>22</sup> T. Tanaka and S. Kashiwaya, Phys. Rev. Lett. **74**, 3451 (1995).

<sup>23</sup> S. Kashiwaya, Y. Tanaka, M. Koyanagi, and K. Kajimura, Phys. Rev. B **53** 2667 (1996).

<sup>24</sup> S. Kashiwaya and Y. Tanaka, Rep. Prog. Phys. **63**, 1641 (2000).

<sup>25</sup> T. Löfwander, V. S. Shumeiko and G. Wendin, Supercond. Sci. Technol. **14**, R53 (2001).

<sup>26</sup> M. Yamashiro, Y. Tanaka, and S. Kashiwaya: Phys. Rev. B **56** (1997) 7847.

<sup>27</sup> M. Yamashiro, Y. Tanaka, Y. Tanuma and S. Kashiwaya, J. Phys. Soc. Jpn. **67**, 3224 (1998).

<sup>28</sup> M. Yamashiro, Y. Tanaka, N. Yoshida and S. Kashiwaya, J. Phys. Soc. Jpn. **68**, 2019 (1999).

<sup>29</sup> C. Honerkamp and M. Sigrist: J. Low. Temp. Phys. **111**, 898 (1998); Prog. Theor. Phys. **100**, 53 (1998).

<sup>30</sup> F. Laube, G. Goll, H. v. Löhneysen, M. Fogelström, and F. Lichtenberg, Phys. Rev. Lett. **84**, 1595 (2000).

<sup>31</sup> Z. Q. Mao, K. D. Nelson, R. Jin, Y. Liu, and Y. Maeno, Phys. Rev. Lett. **87**, 037003 (2001).

<sup>32</sup> C. Wälti, H. R. Ott, Z. Fisk, and J. L. Smith, Phys. Rev. Lett. **85**, 5258 (2000).

<sup>33</sup> K. Sengupta, I. Žutić, H.-J. Kwon, V.M. Yakovenko, and S. Das Sarma, Phys. Rev. B **63**, 144531 (2001).

<sup>34</sup> Y. Tanuma, K. Kuroki, Y. Tanaka, and S. Kashiwaya, Phys. Rev. B **64**, 214510 (2001).

<sup>35</sup> Y. Tanuma, K. Kuroki, Y. Tanaka, R. Arita, S. Kashiwaya and H. Aoki, Phys. Rev. B. **65** 064522 (2002).

<sup>36</sup> Y. Tanaka, Y. Tanuma, K. Kuroki and S. Kashiwaya J. Phys. Soc. Jpn. **71** 2102 (2002).

<sup>37</sup> Y. Tanaka, R. Hirai, K. Kusakabe and S. Kashiwaya, Phys. Rev. B, **60**, 6308 (1999).

<sup>38</sup> Y. Maeno, H. Hashimoto, K. Yoshida, T. Fujita, L.G. Bednorz, and F. Lichtenberg, Nature **372**, 532 (1994).

<sup>39</sup> A. F. Andreev, Zh .Eksp. Teor. Fiz. **46**, 1823 (1964). [Sov. Phys. JETP **19**, 1228 (1964).]

<sup>40</sup> J. X. Zhu, B. Friedman, and C. S. Ting, Phys. Rev. B **59**, 9558 (1999).

<sup>41</sup> S. Kashiwaya, Y. Tanaka, N. Yoshida, and M. R. Beasley, Phys. Rev. B **60**, 3572 (1999).

<sup>42</sup> I. Žutić and O. T. Valls, Phys. Rev. B. **60**, 6320 (1999); **61**, 1555 (2000).

<sup>43</sup> N. Yoshida, Y. Tanaka, J. Inoue, and S. Kashiwaya, J. Phys. Soc. Jpn. **68**, 1071 (1999).

<sup>44</sup> N. Stefanakis, Phys. Rev. B **64**, 224502 (2001); J. Phys. Cond. Matt. **13**, 3643 (2001).

<sup>45</sup> T. Hirai, N. Yoshida, Y. Tanaka, J. Inoue, and S. Kashiwaya, J. Phys. Joc. Jpn. **70**, 1885 (2001).

<sup>46</sup> T. Hirai, N. Yoshida, Y. Tanaka, J. Inoue and S. Kashiwaya, Physica C **367** 137 (2002).

<sup>47</sup> Z. C. Dong, D. Y. Xing, and J. Dong Phys. Rev. B **65**, 214512 (2002)

<sup>48</sup> N. Yoshida, H. Itoh, H. Tsuchiura, Y. Tanaka, J. Inoue, and S. Kashiwaya, Physica C **367** 185 (2002)

<sup>49</sup> N. Yoshida, H. Itoh, T. Hirai, Y. Tanaka, J. Inoue, and S. Kashiwaya, Physica C **367**, 165 (2002).

<sup>50</sup> Z. Y. Chen, A. Biswas, I. Žutić, T. Wu, S. B. Ogale, R. L. Greene, and T. Venkatesan, Phys. Rev. B. **63**, 212508 (2001).

<sup>51</sup> A. Sawa, S. Kashiwaya, H. Obara, H. Yamazaki, M. Koyanagi, Y. Tanaka and N. Yoshida, Physica C Vol.**339**, 107, 2000

<sup>52</sup> H. Kashiwaya, A. Sawa, S. Kashiwaya, H. Yamazaki, M. Koyanagi, I. Kurosawa, Y. Tanaka, and I. Iguchi, Physica C **357-360** 1610 (2001).

<sup>53</sup> C.-C. Fu, Z. Huang, and N.-C. Yeh Phys. Rev. B 65, 224516 (2002)

<sup>54</sup> N. Nagato and K. Nagai, Phys. Rev. B **51** 16254 (1995).

<sup>55</sup> M. Matsumoto and H. Shiba, J. Phys. Soc. Jpn. **64** 3384 (1995), **64** 4867, **65** 2194 (1995).

<sup>56</sup> Y. Ohashi, J. Phys. Soc. Jpn. **65**, 823 (1996).

<sup>57</sup> A. Millis, D. Rainer, and J. A. Sauls, Phys. Rev. B **38**, 4504 (1988).

<sup>58</sup> C. Bruder, Phys. Rev. B. **41**, 4017 (1990).

<sup>59</sup> G. E. Blonder, M. Tinkham, and T. M. Klapwijk, Phys. Rev. B **25**, 4515 (1982).

<sup>60</sup> A. V. Zaitsev, Zh. Eksp. Teor. Fiz. **86**, 1742 (1984); Engl. Transl. Sci. Phys.-JETP (1015) **59**.

<sup>61</sup> A. L. Shelankov, J. Low. Temp. Phys. **60**, 29 (1985).

<sup>62</sup> M. Ashida, S. Aoyama, J. Hara, and K. Nagai, Phys. Rev. **40**, 8673 (1989).

<sup>63</sup> Y. Nagato, K. Nagai, and J. Hara, J. Low Tem. Phys. **93**, 33 (1993).

<sup>64</sup> T. Hirai, Y. Tanaka, and J. Inoue, to be published.

<sup>65</sup> Y. Tanuma, Y. Tanaka, and S. Kashiwaya, Rhys. Rev. B **64**, 214519 (2001).

<sup>66</sup> H. Itoh, Y. Tanaka, J. Inoue and S. Kashiwaya Physica C **367** pp. 99-102 (2002).

<sup>67</sup> Y. Asano, Y. Tanaka and S. Kashiwaya, Phys. Rev. B **65** 064522 (2002).

<sup>68</sup> Y. Tanaka, Y. Nazarov and S. Kashiwaya, unpublished.

<sup>69</sup> N. Yoshida, Y. Asano, H. Itoh, Y. Tanaka, J. Inoue and S. Kashiwaya, unpublished.